A Novel Geometrical Approach to Determining the Workspace of 6-3 Stewart Platform Mechanism

Serdar Ay
Department of Aerospace Engineering
Turkish Air Force Academy
Istanbul,Turkey
say@hho.edu.tr

Abdurrahman Hacioglu
Department of Aerospace Engineering
Turkish Air Force Academy
İstanbul,Turkey
hacioglu@hho.edu.tr

Erguven Vatandas
Department of Aerospace Engineering
Turkish Air Force Academy
İstanbul,Turkey
e.vatandas@hho.edu.tr

Abstract—**This paper presents a novel methodology for the workspace analysis of 6-3 Stewart Platform Mechanism covering all possible leg configurations which need the forward kinematics consideration. The proposed methodology uses a geometrical algorithm to evaluate the position of the movable platform. In this algorithm, the entire achievable positions of the first vertex of the movable platform are defined by considering the constraints of the connected leg lengths and joint angles. The second vertex is determined geometrically by utilizing the linked legs length, and an inverse kinematics approximation gives possible locations for the third vertex. Although it includes the forward kinematics point of view, the suggested method does not require the use of highly nonlinear algebraic equations with multiple solutions and time-consuming iterations which entail good initial values.**

Keywords-Forward and inverse kinematics; workspace analysis; Stewart platform mechanism

I. INTRODUCTION

Stewart Platform Mechanism (SPM) with six degrees of freedom consists of one rigid fixed and one rigid moving platform connected to each other through six variable length legs and joints. Depending on arrangement of legs, SPM is categorized into different types such as 3-3, 6-3, and 6-6.

SPM has been extensively utilized in a wide variety of applications requiring high precision, loading capacity, rigidity and accuracy, such as, flight simulators (Fig. 1) , aligning optics of astronomical telescopes, satellite dish positioning and CNC machining etc.

Figure 1 CN-235 Full Flight Simulator ROKAF (Havelsan) [17].

SPM has limited workspace. Due to these drawbacks, many researchers have focused on this aspect of SPM since the idea of utilizing SPM as a flight simulator was first introduced by D.Stewart [1].

Researchers have determined the workspace of SPM by utilizing either inverse kinematics or forward kinematics. Inverse kinematics of SPM is straightforward contrary to that of the serial mechanisms while forward kinematics is complex. Complexity of forward kinematics arises from its nonlinear feature which naturally leads to a system of highly nonlinear algebraic equations with multiple solutions. Due to this complexity, in the past, many scholars have applied various methods included analytical [2-7], numerical [8-12] and geometrical [13-15] techniques to solve the forward kinematics problem of general SPM. Analytical solutions of forward kinematics require solving a polynomial of degree 16 which results multiple solutions. Numerical approximations usually refer to the Newton-Raphson method which require good initial values and don't always converge at the expected point. For that reason, formulizing forward kinematics through geometric relations presents alternative solution technique.

Describing a geometric approximation with forward and inverse kinematics, this paper proposes a new geometrical method to determine the workspace of 6-3 SPM which includes the entire possible leg configurations. To reflect the workspace of 6-3 SPM, a code is developed in MATLAB to determine location of movable platform. The proposed methodology uses a geometrical algorithm to evaluate the center position of the movable platform. In this algorithm; considering the limitations of the related leg lengths and joints, all possible positions of the first vertex of the moving platform are defined discretely. After that, using the forward kinematics, the second vertex is determined geometrically via the related leg lengths. Finally, an inverse kinematics approximation gives possible locations for the third vertex. Since the entire leg configurations are included discretely for the first vertex,

978-1-4244-9616-7/11/$26.00 ©2011 IEEE

the resulting workspace includes all possible leg configurations which are considered through forward kinematics technique require the forward kinematics consideration. Although it includes the forward kinematics consideration, the suggested method do not require the use of highly nonlinear algebraic equations with multiple solutions and time-consuming iterations which require good initial values and don't always converge at an expected point by considering all mechanical constraints including limitations of the leg lengths and joints.

II. 6-3 STEWART PLATFORM MECHANISM (SPM)

6-3 SPM with six degrees of freedom consists of a rigid moving platform and a rigid fixed platform, as shown in Fig. 2. Both platforms are connected to each other through six variable length legs and spherical joints.

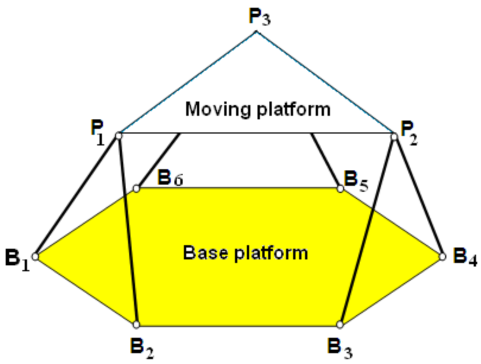

Figure 2. 6-3 Stewart Platform Mechanism.

We consider a 6-3 SPM, the fixed and moving platform of which are equilateral hexagonal and triangle shaped respectively. Leg lengths are L_i varying between L_{imin} and L_{imax}, i=1, 6. The side length of fixed platform is L. The side lengths of movable platform are d_j, j=1, 3. Each pair of the six legs is attached to one vertex of moving platform. B_i and P_j are the centers of the joints located on the fixed and moving platforms, respectively. Geometric relations among vertices P_1, P_2, P_3 and other parameters were presented by Nanua et al. [16].

A. The New Geometrical Methodology

The methodology consists of three steps. In each step, the position of one of the vertices is determined. The details of steps are presented in the following sections:

1) The Determination of Position of Vertex P_1:

The coordinates (p_{1x}, p_{1y}, p_{1z}) of vertex P_1 in Fig. 3 are determined by varying lengths of L_1, L_2 and Φ_1 with respect to the constraints of L_1, L_2, and joints.

L_{bi} and r_j are the distances between B_i and O_j, and between P_j and O_j, respectively, as shown in Fig. 3.

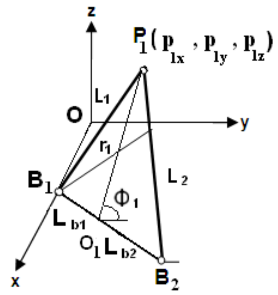

Figure 3. The vertex P_1.

It is necessary to express L_{b1}, L_{b2} and r_1 for vertex P_1 in terms of leg lengths. These expressions include the following:

$$L_{b1} = \frac{L^2 + L_1^2 - L_2^2}{2L} \tag{1}$$

$$L_{b2} = L - L_{b1} \tag{2}$$

$$r_1 = \sqrt{L_1^2 - L_{b1}^2} \tag{3}$$

The coordinates (x_{01}, y_{01}) of O_1 are given by the following equations:

$$x_{01} = x_{b1} + L_{b1}\cos(\pi - \alpha_1) \tag{4}$$

$$y_{01} = y_{b1} + L_{b1}\sin(\pi - \alpha_1) \tag{5}$$

where (x_{b1}, y_{b1}) are the coordinates of B_1 and α_1 is the angle between *x* axis and O_1, as shown in Fig. 4.

The coordinates (p_{1x}, p_{1y}, p_{1z}) of vertex P_1 are given by the following equations:

$$p_{1x} = x_{O1} - r_1\cos\phi_1\sin(\pi - \alpha_1) \tag{6}$$

$$p_{1y} = y_{O1} + r_1\cos\phi_1\cos(\pi - \alpha_1) \tag{7}$$

$$p_{1z} = r_1\sin\phi_1 \tag{8}$$

where Φ_1 determined by considering the limitations of joints is the angle between the planes of *x-y* and the triangle $B_1P_1B_2$. Varying L_1, L_2 and Φ_1 discretely with respect to the related constraints describes the entire achievable positions of the first vertex.

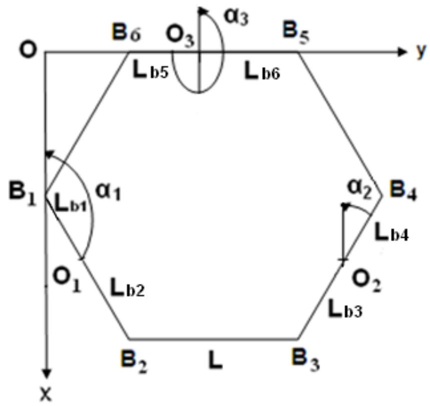

Figure 4. Top view of the rigid fixed platform

2) The Determination of Position of Vertex P_2:

In this phase, the lengths of L_3 and L_4 are varied discretely with respect to the related constraints. The coordinates (p_{2x}, p_{2y}, p_{2z}) of vertex P_2 are determined by considering L_3, L_4, and the coordinates (p_{1x}, p_{1y}, p_{1z}) of vertex P_1 determined in previous phase.

In order to determine P_2 (p_{2x}, p_{2y}, p_{2z}) the geometrical relation between P_1 and P_2 is taken into account. Vertex P_2 may be located on the sphere centered at P_1 with radius d_1, as shown in Fig 5.

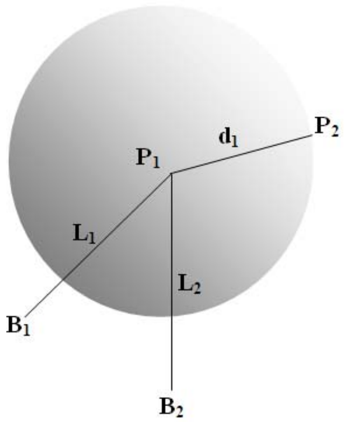

Figure 5. The sphere centered at P_1 with d_1 radius.

Let t be the axis on x-y plane which is perpendicular to the line B_3B_{4a} and passes through O_2 as shown in Fig. 6. Varying lengths of L_3 and L_4 and keeping P_1 fixed, vertex P_2 moves in the circle centered at O_2 with radius r_2, which lies on t-z plane.

In order to determine the coordinates (p_{2x}, p_{2y}, p_{2z}) of vertex P_2, it is necessary to figure out whether or not the sphere centered at P_1 and the circle centered at O_2 intersect.

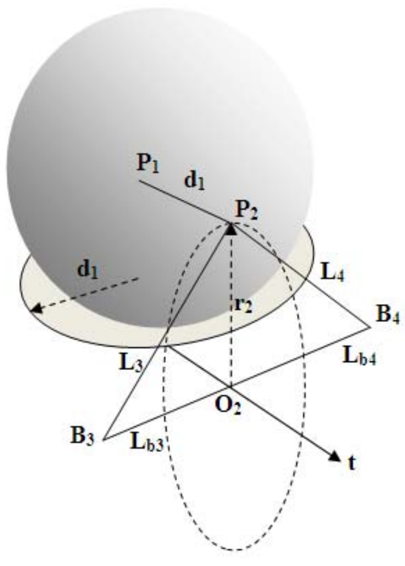

Figure 6. The circle centered at O_2 with radius r_2.

This intersection may exist, providing that the intersection on x-y plane between the projection of the sphere and the axis t exists. The projection on x-y plane of the sphere is the circle centered P'_1 with radius d_1. The axis t can be defined as a line ($y=mx+k$) as shown in Fig.7.

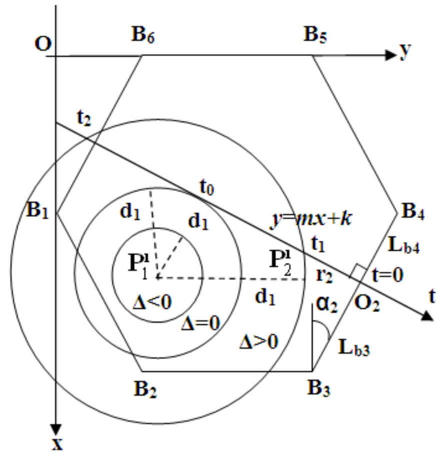

Figure 7. The projections on x-y plane.

The circle with radius d_1 is expressed by the following equation

$$(x - p_{1x})^2 + (y - p_{1y})^2 = d_1^2 \qquad (9)$$

The following equation is written to define the intersection on x-y plane:

$$(x - p_{1x})^2 + (mx + k - p_{1y})^2 = d_1^{\,2} \qquad (10)$$

This quadratic equation possesses two reel roots in the case Δ>0. These reel roots correspond to the point t_1 and t_2 enabling to calculate the radius of the circle located on the t-z plane which is the projection of the sphere centered at P_1. The radius of the circle is given by the following equation:

$$r = \frac{|t_2 - t_1|}{2} \qquad (11)$$

To determine P_2, an additional intersection on the t-z plane shown in Fig. 8 between the circle with radius r and the circle with radius r_2 must be existed. This intersection occurs when the following relation is satisfied:

$$|r - r_2| \le l \le r + r_2 \qquad (12)$$

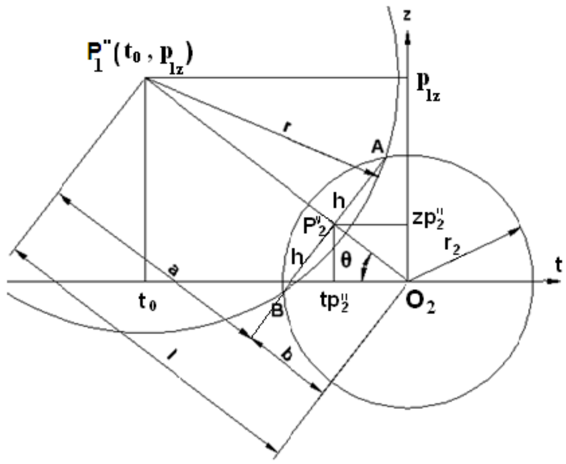

Figure 8. The projections on *t-z* plane.

The radius r_2 of the circle centered at O_2 is given by the subsequent equation;

$$r_2 = \sqrt{L_3^2 - L_{b3}^2} \tag{13}$$

while the distance L_{b3} between B_3 and O_2 (see Fig. 4, 6 and 7) is defined as the following:

$$L_{b3} = \frac{L^2 + L_3^2 - L_4^2}{2L} \tag{14}$$

θ is the angle between the line $P_1''O_2$ and t axis. θ is given by the following equation:

$$\theta = a\tan\left(\left|\frac{p_{1z}}{t_0}\right|\right) \tag{15}$$

where

$$t_0 = \frac{t_1 + t_2}{2} \tag{16}$$

l, a,b and *h* are the distances, as shown in Fig. 8. These expressions include the following relations:

$$l = \sqrt{t_0^2 + P_{1z}^2} \tag{17}$$

$$a = \frac{r^2 + l^2 - r_2^2}{2l} \tag{18}$$

$$b = l - a \tag{19}$$

$$h = \sqrt{r^2 - a^2} \tag{20}$$

The projection on *t-z* plane of vertex P_2 (p_{2x}, p_{2y}, p_{2z}) is $P_2''(tp_2'', zp_2'')$ and tp_2'' , zp_2'' are given by the following equations:

$$tp_2'' = b\cos(\theta) \tag{21}$$

$$zp_2'' = b\sin(\theta) \tag{22}$$

The coordinates of points A and B on *t-z* plane are

$$t_A = tp_2'' + h.\sin(\theta) \tag{23}$$

$$z_A = tp_2'' + h.\cos(\theta) \tag{24}$$

$$t_B = tp_2'' - h.\sin(\theta) \tag{25}$$

$$z_B = tp_2'' - h.\cos(\theta) \tag{26}$$

The coordinates (x_{03}, y_{03}) of O_2 are given by the following equations:

$$x_{02} = x_{b3} + L_{b3}\cos(\pi - \alpha_2) \tag{27}$$

$$y_{02} = y_{b3} + L_{b3}\sin(\pi - \alpha_2) \tag{28}$$

where (x_{b3}, y_{b3}) are the coordinates of B_3. The projections on *x-y* plane of points A and B can be written as

$$x_A = x_{O2} + t_A\sin(\alpha_2) \tag{29}$$

$$y_A = y_{O2} + t_A\cos(\alpha_2) \tag{30}$$

$$x_B = x_{O2} + t_B\sin(\alpha_2) \tag{31}$$

$$y_B = y_{O2} + t_B\cos(\alpha_2) \tag{32}$$

x_A, x_B and y_A, y_B are the solutions of the coordinates (p_{2x}) and (p_{2y}), respectively while z_A and z_B are the solutions of p_{2z}. Each solution of (p_{2x}, p_{2y}, p_{2z}) is accepted for the vertex P_2, if the associated constraints are satisfied.

3) The Determination of Position of Vertex P_3:

Given the coordinates of vertices P_1 and P_2 calculated above, the geometric relations among P_1, P_2, and P_3 are utilized to figure out the coordinates (p_{3x}, p_{3y}, p_{3z}) of vertex P_3.

For a fixed P_1 and P_2, P_3 moves in a circle centered at the point O' with the radius r_0, shown as in Fig. 9.

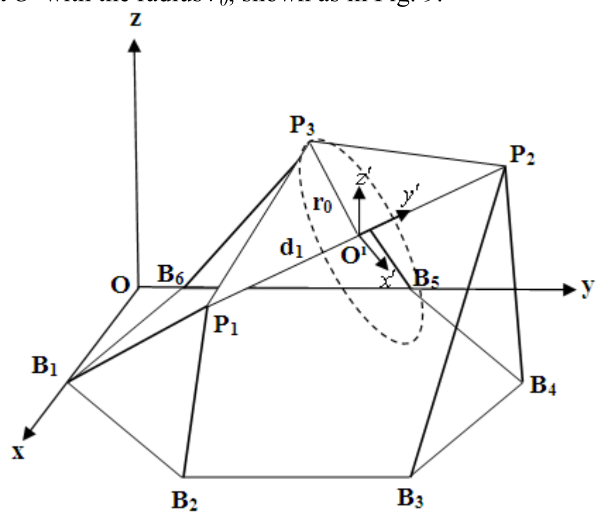

Figure 9. The vertex P3 moving in the circle with radius r_0.

The points on the circle with the radius r_0, where P_3 moves are utilized to determine the leg lengths of L_5 and L_6 through inverse kinematics. Providing that the determined leg lengths satisfy the constraints of the leg lengths and joints, the points are included to the solution set of the vertex P_3. In order to determine vertex P_3, the coordinate frame $O'(x' y' z')$ is defined. The origin of the coordinate frame $O'(x' y' z')$ is located at the center of the circle with the radius r_0 while y' axis passes through the line P_1P_2 and x' axis lying parallel to the x-y plane. P_3 moves along the arc corresponding to the angle φ (in radian). The radius r_0 is given by the following equation with the help of equilateral triangle relation:

$$r_0 = d_1 \frac{\sqrt{3}}{2} \tag{33}$$

The vertex P_3 rotates about y' axis as shown in Fig. 10 and the equation of the circle with the radius r_0 relative to the coordinate frame $O'(x' y' z')$ can be rewritten as

$$(x')^2 + (z')^2 = r_0{}^2 \tag{34}$$

where

$$x' = r_0 \cos\varphi \tag{35}$$

$$z' = r_0 \sin\varphi \tag{36}$$

The coordinates of the origin of $O'(x', y', z')$ are given by the following equations:

$$x'_0 = \frac{(p_{1x} + p_{2x})}{2} \tag{37}$$

$$y'_0 = \frac{(p_{1y} + p_{2y})}{2} \tag{38}$$

$$z'_0 = \frac{(p_{1z} + p_{2z})}{2} \tag{39}$$

The coordinates of the geometric center C (a_0, b_0, c_0) of the moving platform are given by following equations:

$$x_0 = \frac{2x'_0 + p_{3x}}{3} \tag{40}$$

$$y_0 = \frac{2y'_0 + p_{3y}}{3} \tag{41}$$

$$z_0 = \frac{2z'_0 + p_{3z}}{3} \tag{42}$$

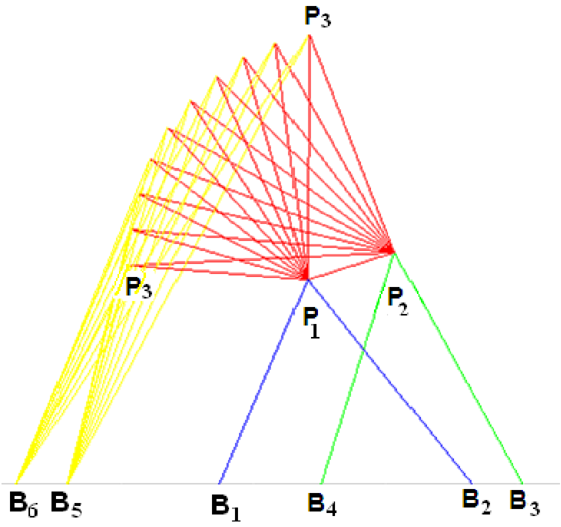

Figure 10. The points reached by vertex P_3.

B_5 and B_6 as shown in Fig. 10 are the points on the fixed platform where L_5 and L_6 are connected, respectively. The coordinates of these points are transformed to the coordinate frame $O'(x' y' z')$. To settle on P_3, the circle is split into Δθ intervals. Using inverse kinematics, the points satisfying all constraints correspond to P_3 (a_3, b_3, c_3).

Determined the coordinates of three vertices, the geometric center of the mobile platform is figured out. That the vertices P_2 and P_3 are evaluated for each achievable position of vertex P_1 results in the workspace.

III. TEST CASE

A 6-3 SPM with L=1 m, d_i=1 m, L_{min}=0.8 m, L_{max}=1.2 m is considered. The joint angle limitation varies between – 45° and 45°. The proposed algorithm results in the workspace in Fig. 11.

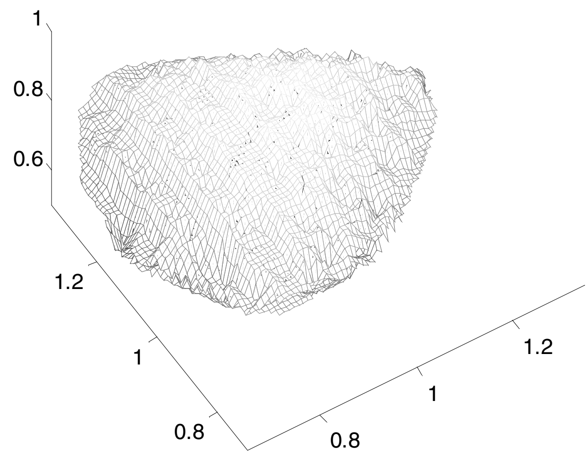

Figure 11. The workspace of 6-3 SPM.

IV. CONCLUSIONS

In this paper, a new geometric method is presented to determine the workspace of 6-3 SPM. Although the entire possible leg configurations are considered to achieve the workspace by using both the forward kinematics and inverse kinematics techniques, the proposed method does not require highly nonlinear algebraic equations with multiple solutions and time-consuming numerical analysis which needs good initial values and doesn't always converge at an expected point by means of all mechanical constraints.

REFERENCES

[1] D.Stewart, "A platform with six degrees of freedom," Proc.Inst.Mech.Eng. vol.180, Pt.1, No.1, pp.371-386, 1965.

[2] J.P.Merlet, "Direct Kinematics of Parallel Manipulators," IEEE Transactions on Robotics and Automation, vol 9(6), pp 842-845, December 1993.

[3] X.Huang, Q.Liao, and S.Wei, "Closed-form forward kinematics for a symmetrical 6-6 Stewart platform using algebraic elimination," Mechanism and Machine Theory, vol.45, pp.327-334, 2010.

[4] J.Enferadi and A.A. Tootoonchi, "A novel approach for forward position analysis of a double-triangle spherical parallel manipulator," European Journal of Mechanics A/Solids, vol.29, pp.348-355, 2010.

[5] D. Gan, Q.Liao, J.S.Dai, S.Wei, and L.D.Seneviratne, "Forward displacement analysis of the general 6-6 Stewart mechanism using Gröner bases," Mechanism and Machine Theory, vol.44, pp.1640-1647, 2009.

[6] C.Zhang and S.M. Song, "Forward Kinematics of a Class of Parallel (Stewart) Platforms with Closed-Form Solutions," Journal of Robotic Systems, vol.9(1), pp.93-112, 1992.

[7] S.Cheng, H.Wu, C.Wang, Y.Yau, and J.Zhu, "The Forward Kinematics Analysis of 6-3 Stewart Parallel Mechanisms," ICIRA 2010, Part I, pp.409-417, 2010.

[8] X.S.Wang, M.L.Hau, and Y.H.Cheng," On the use of differential evolution for forward kinematics of parallel manipulators," Applied Mathematics and Compution, vol.205, pp.760-769, 2008.

[9] Y.Wang, "A direct numerical solution to forward kinematics of general Stewart–Gough platforms," Robotica, vol.25, pp.121-128, 2007.

[10] R.Boudreau and N.Turkkan, "Solving the Forward Kinematics of Parallel Manipulators with a Genetic Algorithm," Journal of Robotic Systems, vol.13(2), pp.111-125, 1996.

[11] Z.Wang, J.He, H.Shang, and H.Gu, "Forward kinematics analysis of a six-DOF Stewart platform using PCA and NM algorithm," Industial Robot,vol.36/5, pp.448-460, 2009.

[12] A.Omran, M.Bayoumi, A.Kassem, and G.El-Bayoumi," Optimal Forward Kinematics Modeling of Stewart Manipulator Using Genetic Algorithms," Jordan Journal of Mechanical and Industrial Engineering, vol.3(4), pp.280-293, 2009.

[13] D.M.Ku, "Direct displacement analysis of a Stewart platform mechanism," Mechanism and Machine Theory, vol.34, pp.453-465, 1999.

[14] S.G.Kumar, T.Nagarajan, and Y.G.Srinivasa, "Characterization of reconfigurable Stewart platform for contour generation," Robotics and Computer Integrated Manufacturing, vol.25, pp.721-731, 2009.

[15] S.K.Song and D.S:Kwon,"New Direct Kinematics Formulation of 6 D.O.F. Stewart-Gough Platforms Using the Tetrahedron Approach," Transactions on Control, Automation, and Systems Engineering, vol.4(3), pp.217-223, 2002.

[16] P. Nanua, K. J. Waldron, and V. Murthy, "Direct kinematic solution of a Stewart platform," IEEE Trans. Rob. Automation,. 6(4), pp.438–444, 1990.

[17] http://www.havelsan.com.tr/SisCoz/ENProjeler.aspx